Quest Journals
Journal of Electronics and Communication Engineering Research
Volume 10 ~ Issue 1 (2024) pp: 01-20
ISSN(Online) : 2321-5941
www.questjournals.org

Research Paper

Maximum Power Point Tracking System For Solar Application Using Fuzzy Logic Controller

Owuamanam Chrysantus .C.[1] Akpado Kenneth .A.[2] Ikpo kingsely .U.[3] Alagbu Ekene .E.[4] Okafor Chukwunenye .S.[5]

[1]Federal Polytechnic Nekede Owerri Department of Electrical Electronics [3] Petroleum Training Institute Effurum, Delta [2,4 and 5]Nnamdi Azikiwe University Department. of Electronic & Computer Engineering Awka, Nigeria.

ABSTRACT
This study presented detailed design, implementation and testing of a prototype Fuzzy logic based Maximum Power Point Tracker (MPPT) charge controller embedded in an 8 bit PIC microcontroller to be used in a standalone Photovoltaic (PV) systems, which is able to monitor the power generated by the photovoltaic array and deliver the maximum amount into charging a lead acid battery under varying atmospheric conditions, while simultaneously monitoring the battery state of charge and ensuring efficient solar to battery power transfer. Prototyping methodology was adopted in this work for speedy development. Physical model is implemented and tested to demonstrate the concept of a fuzzy logic based Maximum Power Point Tracking (MPPT) controller for Photovoltaic battery charging system. A 260W photovoltaic (PV) panel and 12V 50AH battery panel is used to carry out testing of the controller. Variations in solar irradiation resulted in a varying output power from the solar panel, hence varying battery charging power. A maximum average system power conversion efficiency of 91% was observed during the tests. It can be seen that the PV voltage was actively altered by the MPPT charge controller with corresponding changes in PV output current, so as to extract the maximum power available at the persisting solar irradiation. The result obtained showed that the fuzzy logic based MPPT is able to adjust the power point of the solar panel to match the prevailing solar irradiation, and the battery state of charge

***R**eceived 01 Jan., 2024; **R**evised 08 Jan., 2024; **A**ccepted 10 Jan., 2024 © The author(s) 2024.*
P**ublished with open access at **www.questjournals.org

I. Background to the Study

Renewable energy sources are fast becoming an alternative to traditional fossil fuels due to their advantages of being clean and inexhaustible. Solar power is one of the renewable energy sources and although it has a high potential, its generation efficiency (conversion of solar energy to electricity) is low with most commercial solar panels having efficiencies of less than 30% (Dipali, k. et al. 2018). If Maximum Power Point tracking system using fuzzy logic controller is employed, the efficiency can rise as high as 90%. With this already low power generation efficiency of solar panels it is only necessary that the maximum power is sourced from that generated by solar panels to ensure high efficiency in delivering power to the load to make solar power an effective alternative and justify its high installation costs too. (Abonyo, 2016). Renewable energy often referred to as clean energy is energy generated from natural sources or processes that are constantly replenished and includes wind power, solar radiation as well as energy from other naturally and constantly replenished sources (sunlight, rain, wave, tides, geothermal heat, etc). (Renewable energy, 2022).

Researches and development of alternative sources of energy that are clean, efficient, renewable and environmentally friendly were motivated due to the negative effects of climate change that is associated with the use of fossil fuel and rising energy demand of nations. (Renewable energy, 2022).

Photovoltaic (PV) module output power depends on the solar irradiance and the operating temperature; therefore it is necessary to implement Maximum Power Point Tracking (MPPT) controllers to obtain the maximum power of a PV system irrespective of variations in climatic conditions. (Abonyo, 2016).

For maximum efficiency from the solar panel to be attained, it is important to obtain the maximum available power at any operating condition. (Addourraziq and Maaroufi, 2017). This technique is called Maximum Power Point Tracking (MPPT). The PV module maximum output power is dependent on the

operating conditions and varies from time to time due to temperature, load and irradiation. Hence tracking and adjusting for this maximum point is a continuous exercise.

II. Statement of the Problem:

The problem that output power of a photovoltaic (PV) module depends on the solar irradiance and the operating temperature; hence it is important to implement maximum power point tracking (MPPT) controllers to obtain the maximum power of a PV system regardless of variations in climate conditions. Increase in solar irradiation produce increases in the short-circuit current, while increases in temperature decrease the open circuit voltage, which affects the output power of the PV module. This variability of the output power means that in the absence of coupling devices between the PV module and the l.oad, the system does not operate at the maximum power point (MPP).

Controlling MPPT for the solar array is essential in a PV system in order to reduce the cost of yielded electrical energy. This project presents the design, simulation and implementation of a fuzzy controller to track the maximum power point of a PV module using the characteristics of fuzzy logic to represent a problem through linguistic expressions. The fuzzy logic algorithm is used to minimize the error between the actual power and the estimated power.

III. Review of Related Literature

Chendi, Yuanrui, Dongbao, Junfeng & Jun (2016) in their work titled "A High-Performance Adaptive Incremental Conductance MPPT Algorithm for Photovoltaic Systems" analysed existing MPPT methods, and designed a novel incremental conductance (INC) MPPT algorithm with an adaptive variable step size. The algorithm automatically regulated the step size to track the MPP through a step size adjustment coefficient, and a user predefined constant is unnecessary for the convergence of the MPPT method, thus simplified the design of the PV system. A tuning method of initial step sizes was also presented, which is derived from the approximate linear relationship between the open-circuit voltage and MPP voltage. Compared with the conventional INC method, their method can achieve faster dynamic response and better steady state performance simultaneously under the conditions of extreme irradiance changes. A Matlab/Simulink model and a 5 kW PV system prototype controlled by a digital signal controller (TMS320F28035) were established

Another relevant work is that of Algarrin, Giraldo, and Alvenez, (2017) titled "Fuzzy logic based mppt controller for a pv system", presented the design and modeling of a fuzzy controller for tracking the maximum power point of a system. For the implementation, they chose a 65W PV system and used matlab/simulink for the modeling of the components of a 65W PV system. Algarrin et al. (2017) agreed that fuzzy controller is superior in terms of settling time, power loss and oscillations at the operating point. The calculations made apply to PV modules with powers up to 65W. One of the inputs of the fuzzy controller is the change of error, which requires a differentiation operation that increases the complexity in the calculations and can generate errors when measuring small powers that are sensitive to noise.However, the DC-DC converter and fuzzy control were designed based on the electrical parameters of PV module under study. For this reason, the calculations made apply to PV modules with powers up to 65W.

In a work done by Akpado, Okwaraoka and Aririguzo (2017) titled " Design and Implementation of Battery Charge Controller Using Embedded Fuzzy Logic System", fuzzified battery charging was designed and implemented using a PIC16F877A microcontroller. Temperature, voltage and charging current were monitored to fuzzylogically control the Pulse Width Modulated (PWM) output used to deliver the correct charging power. They used a Metal Oxide semiconductor Field Effect Transistor (MOSFET) as a switching device controlled with pulse width modulated (PWM) output of the microcontroller. The implementation of fuzzy logic controller was not done on 8-bit microcontroller

Mostefa & El Madjid (2017) did comprehensive comparative study of the most adopted Artificial Intelligence (AI)-based MPPT techniques in their work titled "Artificial intelligence-based maximum power point tracking controllers for Photovoltaic systems: Comparative study". In this work, they attempted to summarize and to give a comprehensive comparative study of the most adopted Artificial Intelligence (AI)-based MPPT techniques. The MPPT techniques which they described were based on: Proportional-Integral-Derivative (PID), Fuzzy Logic (FL), Artificial Neural Network (ANN), Genetic Algorithms (GA) and Particle Swarm Optimization (PSO). The developed MPPT controllers were tested under the same weather profile in the same photovoltaic system which was composed of a PV module, a DC-DC Buck-Boost converter and a DC load. They initially Modelled and simulated the system using the MATLAB/Simulink environment. Thereafter, the sliding mode control was applied to the converter in order to improve its performance. In a further stage, the different steps of development for each MPPT technique were presented. They performed simulation to confirm the validity of the proposed controllers under the same variable temperature and solar irradiance conditions. Finally, they carried a comparative study in order to evaluate the developed techniques regarding two principal criteria: the performance and the implementation

cost. The performance was evaluated using comparative analysis of the tracking speed, the average tracking error, the variance and the efficiency. To estimate the implementation cost, they carried out a classification according to the type of the used sensors, the type of circuitry and the software level complexity.

Amrouche, Bechemel and Guessoum (2017) in their work titled "Artificial Intelligence Based P&O MPPT", showed the negative effects associated with the conventional control methods such as perturb &observe (P&O) can be greatly reduced if the artificial intelligence (AI) concepts are used, where the perturbation step is continuously approximated by using artificial neural network (ANN) The work showed better steady state and dynamical performance than traditional P&O. However, drawbacks such as slow response speed, oscillation around the MPP in steady state and tracking in wrong way under rapidly changing atmospheric conditions were not totally eliminated.

In a report of similar work titled "Maximum Power Point Tracking In Solar Power Systems By Using Differential Evolution Methods With Embedded Systems" by Volkan and kadir (2017), the MPPT is achieved by optimizing the light intensity vector on a solar panel after measuring the daylight physically with the help of newly designed embedded system and processing the real world values by using differential search algorithm, DSA. They concluded that DSA provides a good solution performance, robustness and superiority and can effectively be used in large scaled, non-linear and non-convex problems in parameter estimation and maximum power point tracking area.They used differential search algorithm to determine the MPPT and position of PV panel. The main disadvantage of the algorithm is that it has increased complexity.

Ibrahim, Ighneiwa and Abdelmeneim (2018) in their work "Using Intelligent Control To Improve PV Systems Efficiency" agrees that photovoltaic (PV) is an important technology in renewable energy. They implemented unconventional techniques, intelligent control to control more than two parameters at a time, including change in temperature. They used probability theory to predict the location of Power Point and control how it would move before not after it did. Ibrahim et al. (2018) agreed that PV systems are the cleanest and the easiest to implement and used three dimensional fuzzy logic controllers with feedback and confirmed the Fuzzy Logic Controller FLC is better than other contemporary control methods. However, the conclusion of the work is based on probability rather than certainty to predict the MPP and take actions before not after the MPP move up or down. The PV module they used has an output peak power (P_m) 50W, open circuit voltage (V_{oc}) 21.6V, short circuit current (I_{sc}) of 3.05 A, irradiance (r) of 1000W/m^2 .

Samosir, Gusmedi, Purwiyanti and Komalasari (2018) of University of Lampung, Indonesia, in a work titled ''Modelling and Simulation of Fuzzy Logic based Maximum Power Point Tracking (MPPT) for PV Application '' modelled and simulated a Fuzzy Logic based Maximum Power Point tracking for PV Application. This work is worth a mention because the report clearly developed and tested a simulation model to investigate the effectiveness of the MPPT controller. The PV module they considered in simulation is 1CA100. They used centre of Area (gravity) defuzzification method. 1CA 100 PV module produces power with maximum power voltage of around 17.6V on a very hot day 25^0C, it can drop to around 16V on a very hot day and it can also rise to 19V on a very cold day.

Akpado et al. (2018) presented a fuzzy logic based algorithm for intelligent air conditioning system. The designed system consists of two sensors for feedback control: one to monitor temperature and another one to monitor humidity. The logic control was developed to control the operation mode of the air conditioning, and maintain the room set conditions. A fuzzy rule for this controller was formulated by temperature and humidity. A fuzzy rule for this controller was formulated by temperature and humidity.

Dmitry, Saad, Yoash, & Juri (2019) in their paper titled "Improved Fractional Open Circuit Voltage MPPT Methods for PV Systems" proposed two new Maximum Power Point Tracking (MPPT) methods which improve the conventional Fractional Open Circuit Voltage (FOCV) method. They used a switched semi-pilot cell for measuring the open-circuit voltage. In the first method this voltage was measured on the semi-pilot cell located at the edge of PV panel. During the measurement the semi-pilot cell was disconnected from the panel by a pair of transistors, and bypassed by a diode. In the second Semi-Pilot Panel method the open circuit voltage was measured on a pilot panel in a large PV system. The proposed methods were validated using simulations and experiments. They established that both methods can accurately estimate the maximum power point voltage, and hence improve the system efficiency.

IV. METHODOLOGY:

Prototyping methodology was adopted in this work for speedy development. Physical model is implemented and tested to demonstrate the concept of a fuzzy logic based Maximum Power Point Tracking (MPPT) controller for Photovoltaic battery charging system. A 260W photovoltaic (PV) panel and 12V 50AH battery panel is used to carry out testing of the controller.

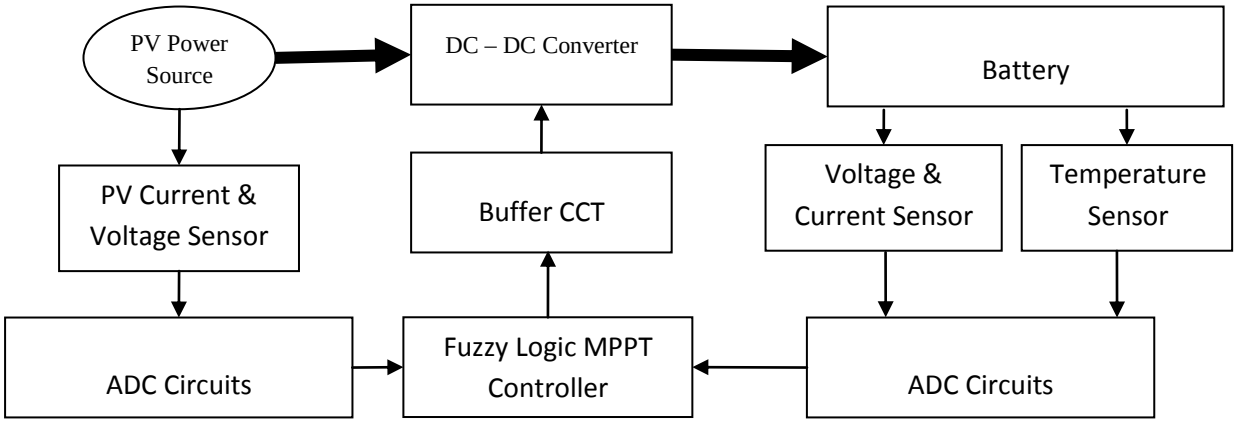

Figure 1: Block Diagram of Fuzzy Logic MPPT controllers

Figure 1 shows the structure of the fuzzy logic controlled PV MPPT controller for battery charger system. The PV power source is a 260W solar panel. The power output of the PV is fed to the battery under charge, through a DC-DC power converter whose output voltage is controlled by the fuzzy logic controlled PV MPPT controller. The fuzzy logic controlled PV MPPT controller will measure the PV output voltage/current and battery voltage, current and temperature using the inbuilt ADC of the microcontroller.

The duty cycle of the DC-DC converter will be controlled by the fuzzy logic controlled PV MPPT controller, using a buffer circuit capable of driving the switching transistors.

4.1 PV POWER SOURCE

The PV power source used to test the fuzzy MPPT solar controller is a 260W solar panel with the following Specification;

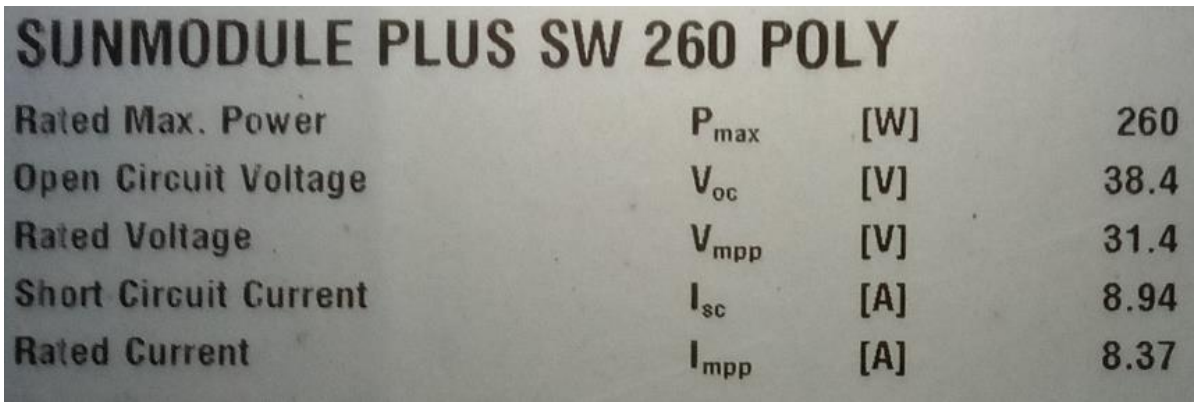

Figure 2: Name Plate specification of the PV Module

From fig. 2, the PV module can produce a short circuit current of 8.94A, and an open circuit voltage of 38.4V. It is rated (or maximum power) voltage and current are 31.4V and 8.37A respectively.

4.2 DC – DC CONVERTER

Table 1 Converter Specification

Input Voltage (V_{IN}):	15 – 60V
Output Voltage (V_{OUT}):	14.4V Maximum
Max Output Current ($I_{OUT_{MAX}}$):	20A Maximum
Switching Frequency (f_{SW}):	25Khz

Synchronous buck converter is chosen in this project for improved power conversion efficiency. As presented in figure 3.3, the converter is comprised of a MOSFET switch(Q1) whose average DC output is varied by the Fuzzy logic controller using pulse width modulation (PWM) technique and filtered by a low pass LC

filter. Given a specific charging voltage requirement computed to maintain maximum power output from the PV module. The MOSFET switch Q2 is connected in the place of a freewheeling diode (as used in regular buck converters) to reduce power dissipation and hence improve overall conversion efficiency.

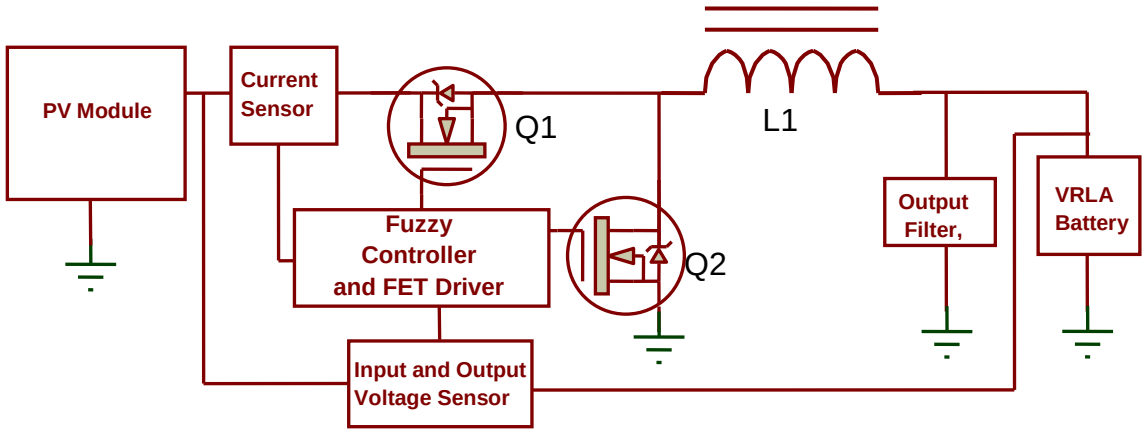

Figure 3 The Synchronous buck converter block diagram

4.3 MOSFET Selection;

Since the worst case input voltage-$V_{in_{Max}}$ is 60V, Q1 must be able to block this voltage. The maximum output current - $I_{OUT_{Max}}$ specified in this model is 20A at output voltage-V_{OUT} of 14.4V. This means that at the maximum expected input current through Q1 will never exceed 20A, and the converter output voltage is never allowed to exceed the input voltage, therefore isolation relay is provided at the PV input.

The switch Q2 being a replacement for freewheeling diode in this configuration is expected to handle the maximum ripple and average current of the inductor - L1 as well as block the input voltage. Therefore Q2 and Q1 should have similar parameters. An Infineon advanced HEXFET power MOSFET IRF3710 was selected for this application. From the datasheet, It has 100V_{DS} and 57A, at 23mΩ R_{DSON}, it will provide reasonably high efficient switching capability.

4.4 Inductor Selection;

Inductor L1 is selected under the assumption of zero on resistance for Q1 and Q2,

$$L = (V_{IN_{MAX}} - V_{OUT}) \times \frac{V_{OUT}}{V_{IN_{MAX}}} \times \frac{1}{f_{SW}} \times \frac{1}{LIR \times I_{OUT_{MAX}}} \quad - \quad - \quad (3.1)$$

Where LIR represents ratio of peak inductor current-$I_{\triangle Lp\text{-}p}$ to maximum output current-I_{OUTMax}.

i.e LIR = $I_{\triangle Lp\text{-}p}$ / I_{OUTMax}

Assuming allowable inductor ripple current $I_{\triangle Lp\text{-}p}$ of 0.5$A_{p\text{-}p}$, the calculated inductance of the inductor is approximately 106uH.

4.5 ADC CIRCUITs

An Analogue to Digital Converter (ADC) takes the analogue signals from the analogue sensors *(Input Current, Input Voltage, Output Voltage and Temperature sensor circuits)* of the MPPT DC-DC system and converts them to digital equivalents for the fuzzy controller module.

Input and Output Voltage Sensors;

(a) Input (b) Output

Figure 4 Circuit diagram of Input and Output voltage Sensor

The resistor network shown in figure 3.4 is used to attenuate the input and output voltage to a value slightly lower than the maximum input voltage of ADC, which is 5VDC. The 8bit PIC microcontroller used in this work has an integrated ADC input with a resolution of 10bits. Therefore there are 2^{10} possible input voltage steps that can be recognized by the ADC. This means that we can measure the voltages with a resolution of 4.88mV approximately.

Using the voltage divider rule;

$$V_{in\_s} = V_{in_{MAX}} \left(\frac{R1}{R1+R2}\right) \quad \text{.....(3.2)}$$

Where $V_{in_{MAX}}$ =60V, and current through R1 and R2 is 0.45mA. Assuming the ADC input has infinite input impedance and the maximum allowed ADC input voltage set at 4.5V. R1 is approximately 123KΩ, while R2 is 10KΩ variable resistor.

In the same vein, assuming maximum V_{OUT} to be 15V (suitable for charging a 12V battery), and corresponding maximum ADC input voltage of 4.5V, then R3 and R4 are approximately 24k and 10K variable respectively.

The DC-DC converter uses a high-side current sensing arrangement, implemented with an ACS712T hall sensor rated for 30A bidirectional current flow.

An LM35 temperature sensor is used to measure the ambient temperature. Figure 3.5 shows the schematics of LM35 circuit connection to the microcontroller. From the data sheet, LM35 can measure -55^{o}C to 150^{o}C range of temperature, making it suitable for this demonstration, as VRLA battery manufacturers quote operating temperature well within this range. For this work, a temperature safe zone of 0 to 50^{o}C is assumed.

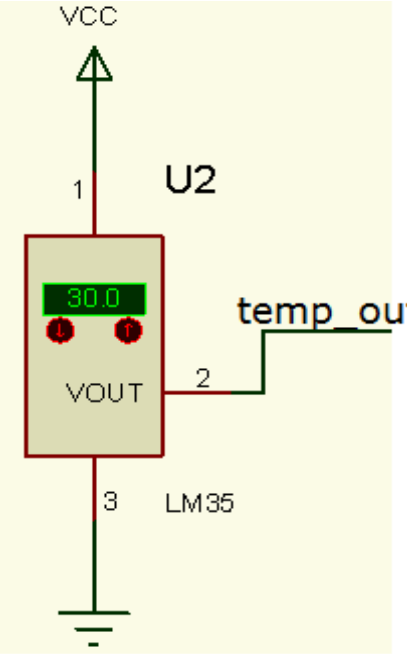

Figure 5 Proteus Schematic of LM35 Connection

4.6 BUFFER CIRCUIT AND EMBEDDED FUZZY LOGIC CONTROLLER

This is the driver circuit for the MOSFET switches; it takes the control signal output of the fuzzy controller and use it to drive the DC switching MOSFETs Q1 and Q2. MOSFET driver chip - IR2110 is used to implement the gate driver of IRF3710. In this work, the fuzzy logic controller is embedded in PIC16F690 microcontroller. The structure of the fuzzy process is shown in Figure 3.6;

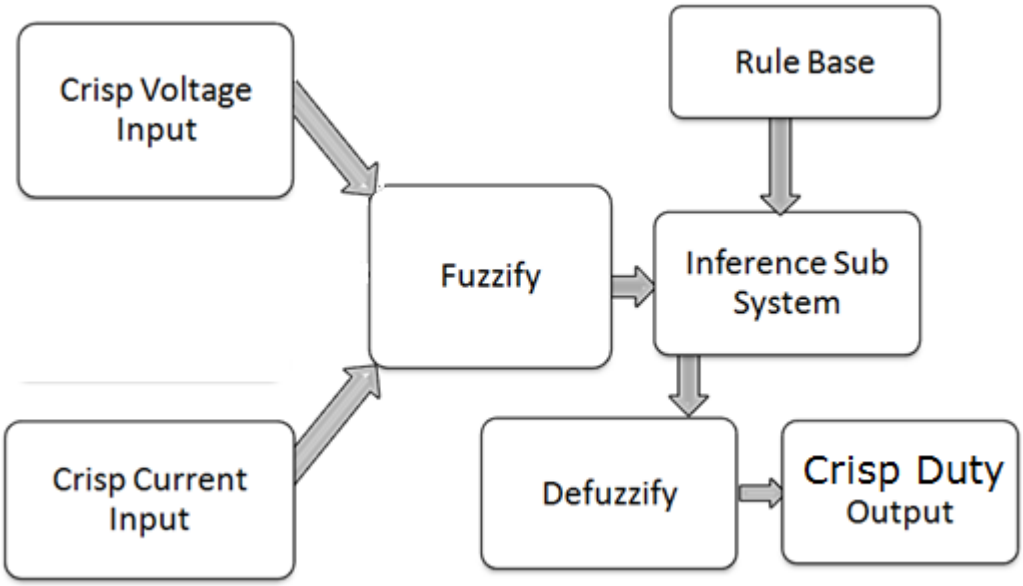

Figure 6. Fuzzy logic Structure

4.7 Crisp Voltage Input

This is the voltage sampled directly from the PV module using the voltage divider shown in Figure 3.4, the maximum voltage is 4.5V, while the minimum is 0V. Therefore the system must map this 0-4.5V range to PV and battery voltage ranges of 00 – 60V and 0-15V respectively.

Table *3.1* shows voltage level mapping by the microcontroller ADC output, scaled up to get actual PV and battery voltages after measurement.

From the datasheet of PIC16F690, the internal ADC has 10 bit resolution, and uses two registers to store results - A/D Result High Register (ADRESH) and A/D Result Low Register (ADRESL).

Table 3.2 does not show the full resolution of the measurement made by the ADC, but shows the estimated value of full voltage range which the system is required to measure. The shaded range indicates the allowed operating range of the controller with respect to various input voltage ranges.

Table 2 Voltage Mapping by Microcontroller ADC

PV Voltage (V_{PV})	**Battery Voltage (V_{BAT})**	**Voltage Divider Output (V_{ADC})**	**ADC Value (V_{ADC}*1024/VCC)**	
			Decimal	***HEX***
66.67	16.6	5.00	1023	3FF
60.00	15	4.50	922	399
58.00	14.5	4.35	891	37A
54.00	13.5	4.05	829	33D
52.00	13	3.90	799	31E
48.00	12	3.60	737	2E1
44.00	11	3.30	676	2A3
42.00	10.5	3.15	645	285
40.00	10	3.00	614	266
36.00	9	2.70	553	228
32.00	8	2.40	492	1EB
28.00	7	2.10	430	1AE
24.00	6	1.80	369	170
20.00	5	1.50	307	133
16.00	4	1.20	246	F5

12.00	3	0.90	184	B8
8.00	2	0.60	123	7A
4.00	1	0.30	61	3D
0.00	0	0.00	0	0

PV Voltage (V_{PV}) is the possible range of voltage that the PV can produce. **Battery Voltage (V_{BAT})** is the range of possible voltages that can be applied while charging or discharging a 12 volts battery. The **Voltage Divider Output (V_{ADC})** is the expected voltage output from the voltage sensors shown in figure 3.4, while the **ADC Value** column shows the values that will be presented to the proposed fuzzy logic controlled PV MPPT controller by the built in ADC of the PIC16F690 microcontroller for the corresponding voltages produced by the voltage sensors.

Crisp Current Input

Sample of the input current measured with the ACS712 circuit is the crisp current input, which is converted by the ADC in the microcontroller. The current value is increased or reduced in response to changes in the PV output power, with a view to maintaining the maximum possible output power (MPPT), by altering the duty cycle of the PWM signal driving the MOSFETs from the microcontroller.

High-side sensing is desirable, as it is considered better than low side sensing so that it directly monitors the current delivered to the battery by the supply. This will ease detection of any short circuit in the system and prevent damages.

The current sensing arrangement is as shown in figure 3.7;

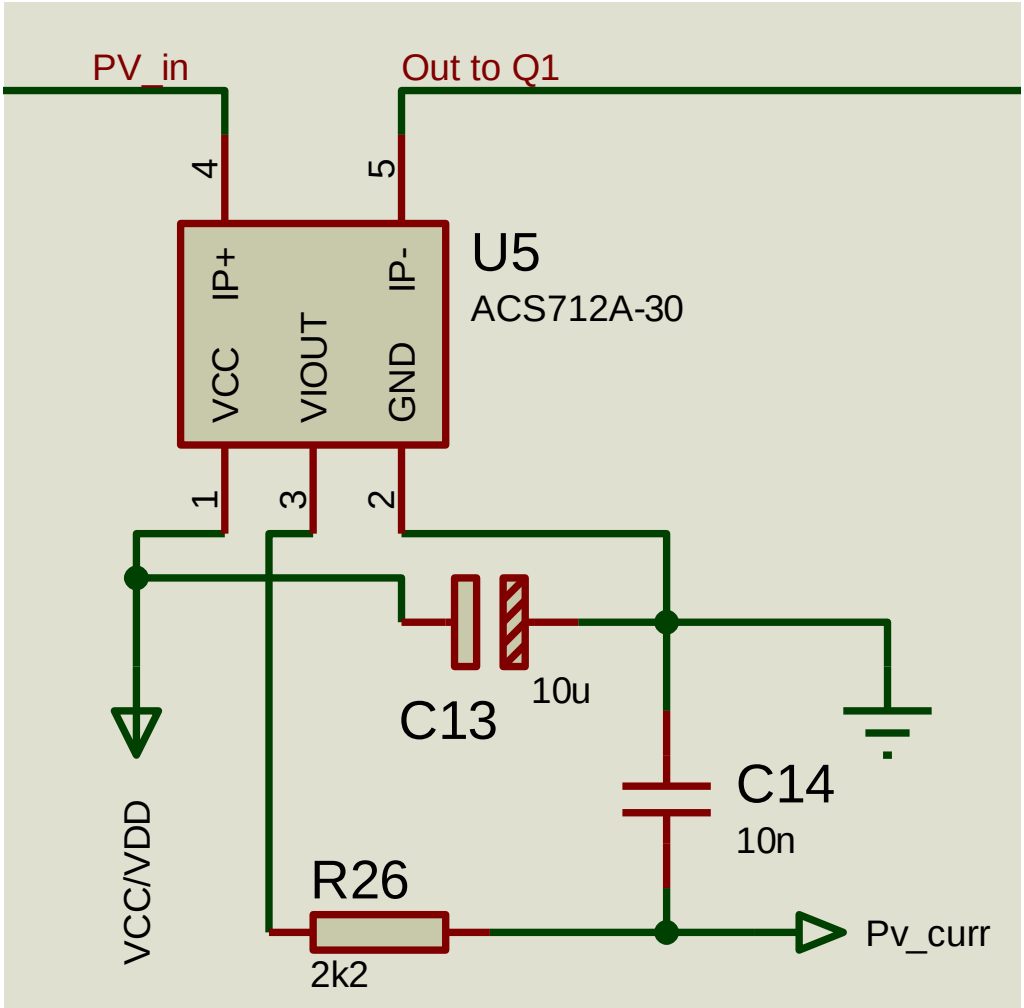

Figure 7 Current measurement using a resistor

The RC low pass filter made up of R26 and C14 has a cutoff frequency (f_o) of approximately 7.2KHz (see equation 3.3). This ensures that the ripple current resulting from the 25Khz switching frequency is filtered out, while allowing an adequate amount of output current to charge the input of the microcontroller ADC.

$$f_0 = \left(\frac{1}{2\pi RC}\right) \text{.....(3.3)}$$

From the datasheet of ACS712-30, the Quiescent output voltage is VCC/2, therefore, the expected output of the current sensor is 2.5V, when no current is flowing, since the VCC here is 5V. The datasheet also stated sensitivity of this current sensor as 66mV/Ampere, this implies that the ADC with a resolution of 4.88mV can only read a minimum current of approximately 77mA and in similar increments subsequently.

Table 3 ADC Current readout

INPUT CURRENT (AMPS)	**ACS712 Output (V)**	**ADC OUTPUT**	
		Decimal	**Hex**
0	2.50	512	0200
1	2.57	526	020D
2	2.63	539	021B
3	2.70	553	0228
4	2.76	566	0236
5	2.83	580	0243
6	2.90	593	0251
7	2.96	607	025E
8	3.03	620	026C
9	3.09	634	0279
10	3.16	647	0287
11	3.23	661	0294
12	3.29	674	02A2
13	3.36	688	02AF
14	3.42	701	02BD
15	3.49	715	02CA
16	3.56	728	02D8
17	3.62	742	02E5
18	3.69	755	02F3
19	3.75	769	0300
20	3.82	782	030E

Design of the membership functions (mf)

MATLAB and Fuzzylite was used in designing the membership function of the two linguistic variables, Voltage and Current. The temperature reading is used for compensation of the charging voltage after the fuzzy control system has made a decision.

The algorithm used in this work is **Perturb and Observe,** in this method the following steps are executed to find a new maximum power output;

1. Measure the input Voltage v(k),
2. Measure the input Current i(k),
3. Compute the present input Power p(k) = v(k) * i(k),
4. Repeat step 1 to 3 after storing old values as v(k-1), i(k-1) and p(k-1) respectively.
5. Compute Change in input voltage dV = v(k) - v(k-1),
6. Compute Change in input power dp(k),
7. Use the Fuzzy inference system to determine the new Duty cycle (D).

PV VOLTAGE INPUT MF

The battery is assumed fully discharged for a 12V battery, when terminal voltage drops to about 10.5V, and fully charged if the charging voltage is at 14.4V while charging current has dropped to below 1 ampere.

The MPPT function is mostly applicable while the battery is still in bulk mode. In this mode, the PV voltage is adjusted by the controller to produce the maximum possible power.

In this MF, change in voltage dV is ranged from 0 – 5V. Table 3.4 shows the fuzzification of dV range using triangular MF, while figure 3.8 shows the plot of the MFs of the linguistic variable voltage.

Table 4 Linguistic Values for PV Voltage

Change in Voltage (dV) Ranging from 0 to 5V	**Linguistic Classification**	**Linguistic Acronym**
<1.25	VERY SMALL	VS
0 to 2.5	SMALL	SL
1.25 to 3.75	NORMAL	NM
2.5 to 5	LITTLE BIG	LB
>3.75	VERY BIG	VB

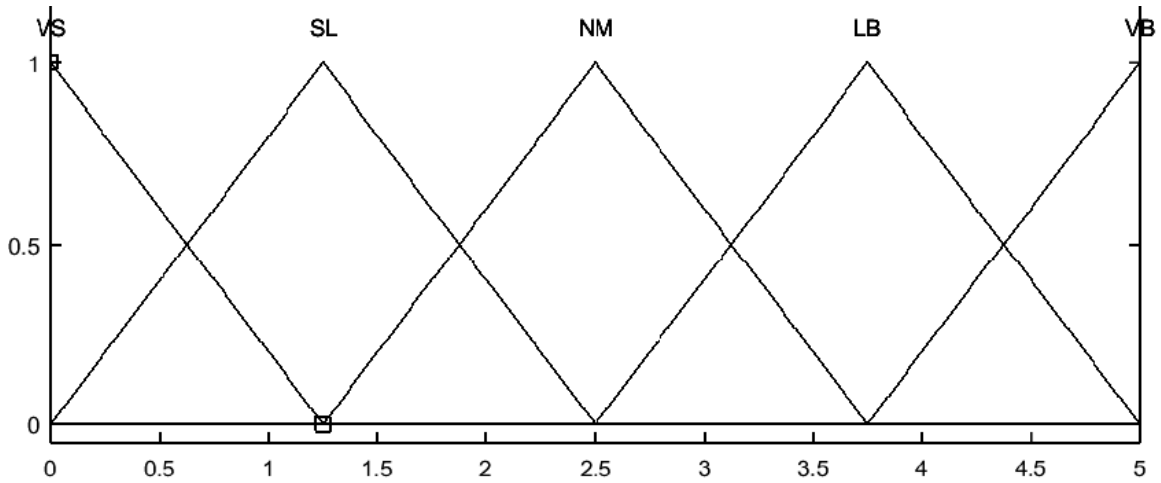

Figure 8 MF plot of change in Voltage dV

3.3.2 PV POWER OUTPUT MF

The Linguistic variable power is derived from the product of PV voltage and output current, as described under the system algorithm in section 3.3. Table 3.5 and figure 3.9 shows the ranges and plot of the MFs in the linguistic variable power.

Table 5 Linguistic Values for PV power

Change in Power (dp) Ranging from 0 to 10V	**Linguistic Classification**	**Linguistic Acronym**
<2.5	VERY SMALL	VS
0 to 5	SMALL	SL
2.5 to 7.5	NORMAL	NM
5 to 10	LITTLE BIG	LB
>7.5	VERY BIG	VB

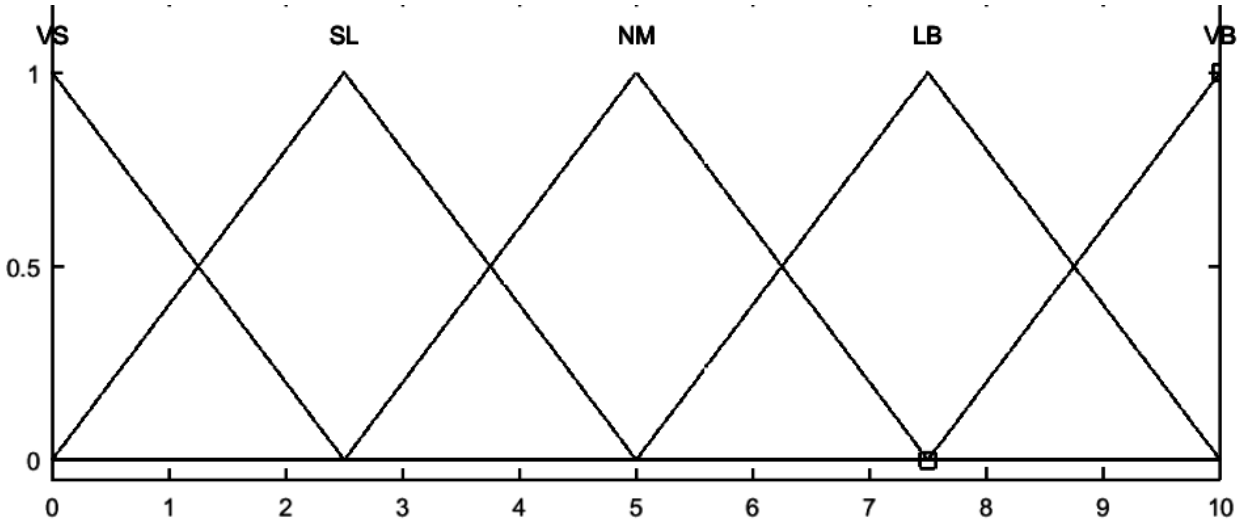

Figure 9 MF plot of change in Power (dp)

FUZZY OUTPUT MF

In PV modules at a given insolation, as load current increase in the module, its terminal voltage decrease and as load current decreases terminal voltage increases.

This PV load current (Battery charging current) is controlled by adjusting the duty cycle of the PWM signal, controlling the DC-DC converter output.

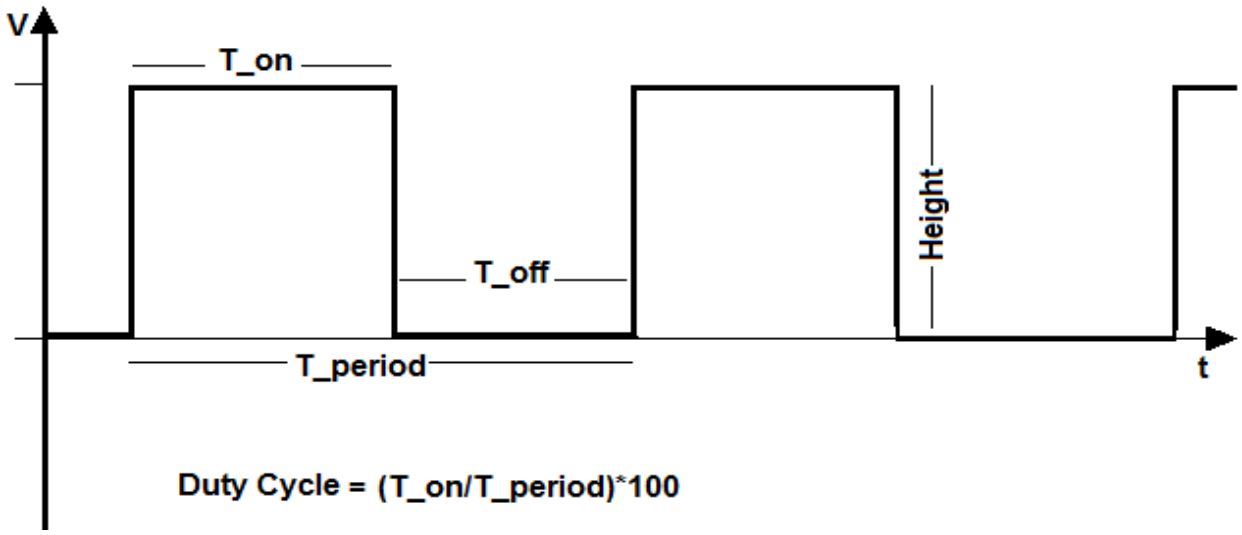

Figure 10 Section of a PWM signal

Figure 3.10 shows a section of PWM signal and the parameters that can be modified to change the average output value.

The change in Duty cycle will be triggered by the value deciphered from the defuzzified output of the controller. A table of the fuzzified output and MATLAB plot of output MF is shown in table 3.6.

Table 6 Fuzzified Output Duty Cycle

Duty Cycle (D) Ranging from 0 to 10V	**Linguistic Classification**	**Linguistic Acronym**
<2.5	REDUCE BIG	RB
0 to 5	REDUCE SMALL	RS
2.5 to 7.5	NORMAL	NM

5 to 10	INCREASE SMALL	IS
>7.5	INCREASE BIG	IB

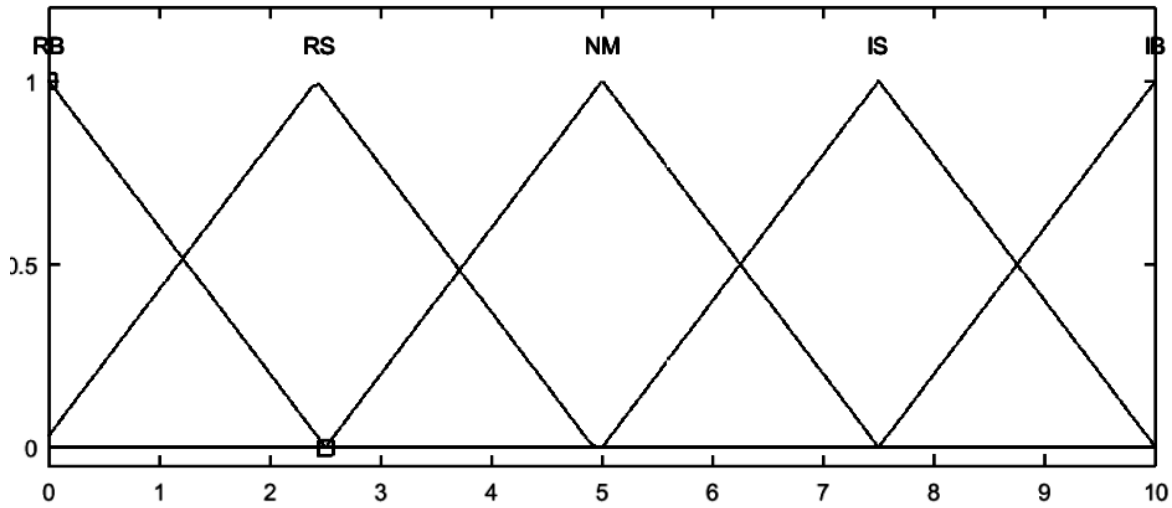

Figure 11 MATLAB plot of Output Duty Cycle Membership functions

As described in table 3.6, the fuzzy duty cycle output of the controller indicates an increase or decrease instruction and how the increase should take place.

RULE BASE DESIGN AND OPERATION

The rule base is organized to ensure that the PV output power stays at it maximum all through the bulk charging stage of the battery. The three stage charging is mimicked, with temperature compensation implicitly applied.

If the battery voltage reaches absorption voltage of 14.4V for VRLA batteries, the MPPT algorithm exits, and a constant output voltage operation is started, when the absorption current has dropped to a preset value between 1 and 2 amperes, the system drops the battery voltage to a float voltage of 13.8V.

Figure 3.12 shows the rule base design taking into accounts an expert knowledge of MPPT implementation using perturbs and observe algorithm.

Duty Cycle		dV				
		VS	SL	NM	LB	VB
dP	VS	IS	IB	RB	RB	RS
	SL	IS	IS	RS	RS	RS
	NM	NM	NM	NM	NM	NM
	LB	RS	RS	IS	IS	IS
	VB	RS	RB	IB	IB	IB

Figure 3.12 Rule Base design of the system.

The Complete Fuzzy Inference System (FIS) Code

The following is the code listing for the fuzzy system in fuzzy inference system format of MATLAB.

```
[System]
Name='Fuzzy MPPT charger'
Type='mamdani'
Version=2.0
NumInputs=2
NumOutputs=1
NumRules=25
AndMethod='min'
OrMethod='max'
ImpMethod='min'
```

```
AggMethod='max'
DefuzzMethod='mom'

[Input1]
Name='dV'
Range=[0 5]
NumMFs=5
MF1='VS':'trimf',[-1.25 0 1.25]
MF2='SL':'trimf',[0 1.25 2.5]
MF3='NM':'trimf',[1.25 2.5 3.75]
MF4='LB':'trimf',[2.5 3.75 5]
MF5='VB':'trimf',[3.75 5 6.25]

[Input2]
Name='dp'
Range=[0 10]
NumMFs=5
MF1='VS':'trimf',[-2.5 0 2.5]
MF2='SL':'trimf',[0 2.5 5]
MF3='NM':'trimf',[2.5 5 7.5]
MF4='LB':'trimf',[5 7.5 10]
MF5='VB':'trimf',[7.5 10 12.5]

[Output1]
Name='D'
Range=[0 10]
NumMFs=5
MF1='RB':'trimf',[-2.5 0 2.5]
MF2='RS':'trimf',[-0.07937 2.421 4.921]
MF3='NM':'trimf',[2.5 5 7.5]
MF4='IS':'trimf',[5 7.5 10]
MF5='IB':'trimf',[7.5 10 12.5]
[Rules]
1 1, 4 (1) : 1
1 2, 5 (1) : 1
1 3, 1 (1) : 1
1 4, 1 (1) : 1
1 5, 2 (1) : 1
2 1, 4 (1) : 1
2 2, 4 (1) : 1
2 3, 2 (1) : 1
2 4, 2 (1) : 1
2 5, 2 (1) : 1
3 1, 3 (1) : 1
3 2, 3 (1) : 1
3 3, 3 (1) : 1
3 4, 3 (1) : 1
3 5, 3 (1) : 1
4 1, 2 (1) : 1
4 2, 2 (1) : 1
4 3, 4 (1) : 1
4 4, 4 (1) : 1
4 5, 4 (1) : 1
5 1, 2 (1) : 1
5 2, 1 (1) : 1
5 3, 5 (1) : 1
5 4, 5 (1) : 1
5 5, 5 (1) : 1
```

COMPLETE CIRCUIT SCHEMATICS OF THE SYSTEM

The complete circuit schematics of the system designed is shown in appendix 1. LEDs indicators show the user the status of the system. LEDs were used for the display because they will demand less resource from the microcontroller, and free up resources for the computations for the fuzzy control system, while keeping the overall cost low.

LED-GREEN shows presence status of the battery. LED-BLUE tells the user battery is charging when it is blinking, but stops blinking to alert the user of completion of charging. LED-RED indicates the presence of PV voltage when it is on.

The LEDs are Standard ones with forward voltage drop of 1.2V and maximum forward current of 10mA. The series resistors of the LEDs R13, R24 and R25 are set to 2.2kΩ to limit the LED forward current to about 1.7mA, thereby reducing power loses to a minimum and elongating the life span of the LEDs.

The datasheet of the PIC16F690 specified the values used for the oscillator and reset circuits.

Algorithm used for the coding

Designing the embedded C language version followed the algorithm below;

1. Get the crisp inputs to fuzzy controller – pvvoltage (***volt***), pvcurrent (***current***)and battery voltage, current and temperature (***temp***)
2. Compute ***fdv***[i] ,***fdp***[j] for all i=0-4and j=0-4, (Find the values of all membership functions given the crisp values. The values of μ is scaled from 0 – 1 to 0 -255)
3. Find the rules that has been fired by searching for the index of first non zero entry in the membership function values stored in arrays fdv[5], fdp[5] and assign these first non zero indexes to the variables ***ist*** and ***jst*** respectively.
4. Compute ***prem***[ist,jst] = ***MIN***(***fdv***[ist], ***fdp[***jst]) for all;

[1]	ist	jst
[2]	ist+1	jst+1
[3]	ist+1	jst
[4]	ist+1	jst+1

5. Find the minimum of each set of premise values for all 4 combinations of fdv[], fdp[]. ***Making sure that index does not overshoot the size of each array***
6. Compute the list of implied output fuzzy sets (***fdutcy***[6]) ***imp_rule***[ist,jst] from the rule base *(shown in Figure 3.12 below)*.

(This should now contain the list of output MF implied by the 4 groups of fuzzy sets in the fired rules)

7. compute index of output MF with the maximum implication ***index_fdutcy*** = ***index_prem***(***max***(prem[ist,jst,kst]))

(Find the index of the maximum value inside prem[ist,jst] and store in ***index_fdutcy***.

8. Compute ***dutcy***=***defuzzify***(***fdutcy***[index_fdutcy]) as the crisp output

(find Mean of Max of the selected fuzzy set by selecting the middle value of the implied output fuzzy set).

9. Send crisp dutcy to the DC-DC switch.
10. Restart the process from step 1.

PCB layout of the circuit

Printed Circuit Board (PCB) of the circuit schematics was prepared using the Ares bundle application inside Proteus 8 Professional software. See Appendix 4 for the picture of the PCB layout and 3D rendering of the circuit board. The PCB was etched using Feric Chloride.

3.5 Corel Draw Rendition of the Prototype Packaging

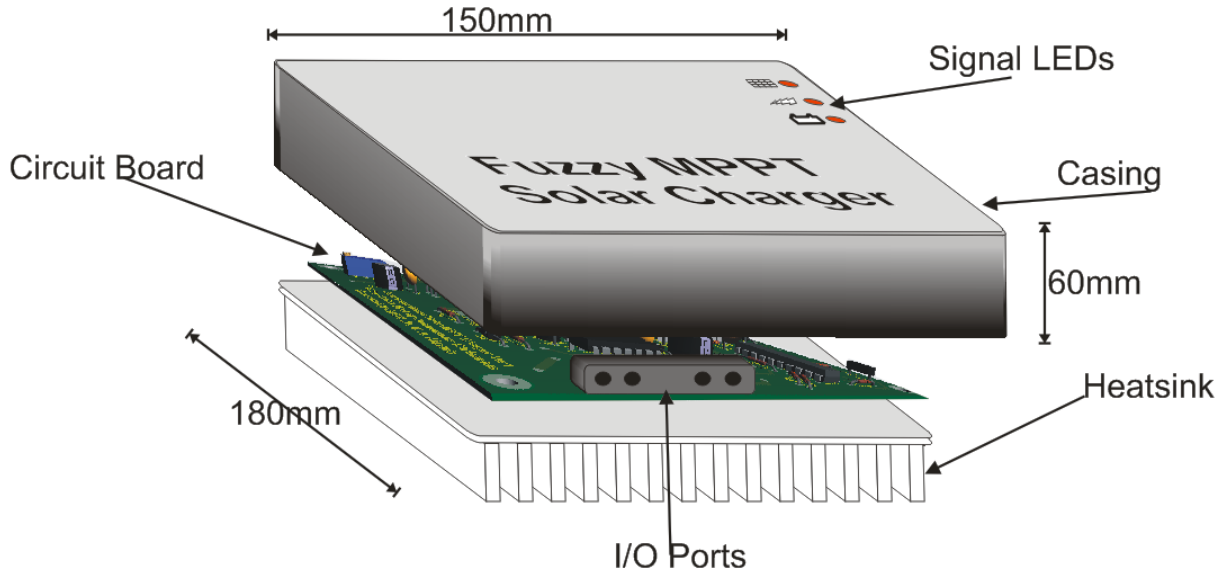

Fig 12 Rendition of the Casing.

V. RESULTS AND DISCUSSION

A surface plot of the variations in solar panel output power (dP) and voltage (dV) versus duty cycle (D) of the system is shown in figure 4.1(a) and (b) below. Performance of the system under mean of max (MOM) and Centroid defuzzification methods, (see figure 13(a) and figure 13 (b) respectively) clearly show a disparity in the smoothness of curve.

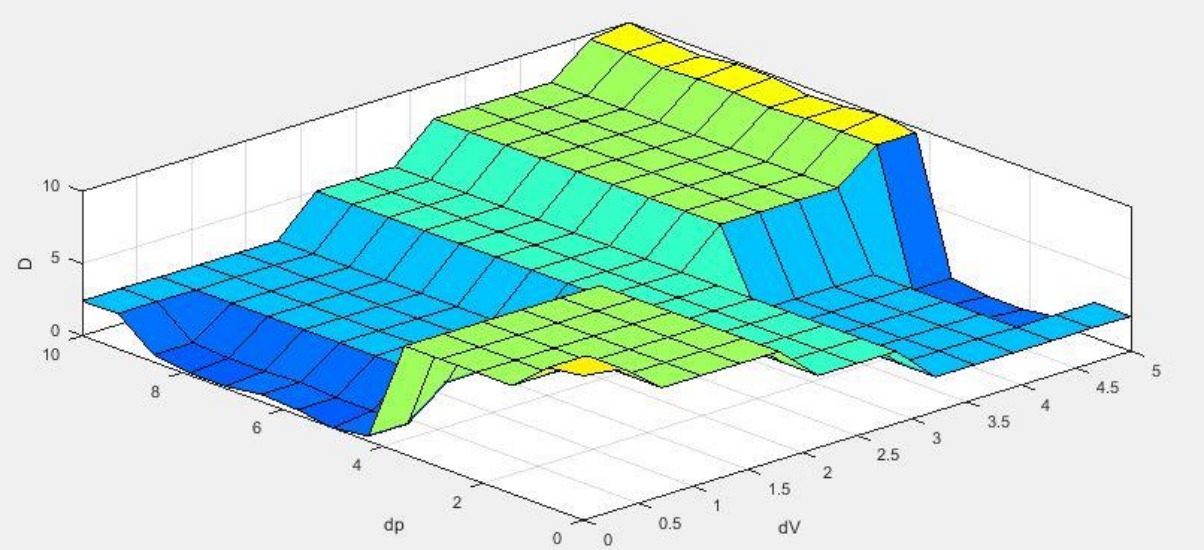

Figure 13(a) Variation of D with changes in dP and dV using MOM defuzzifier.

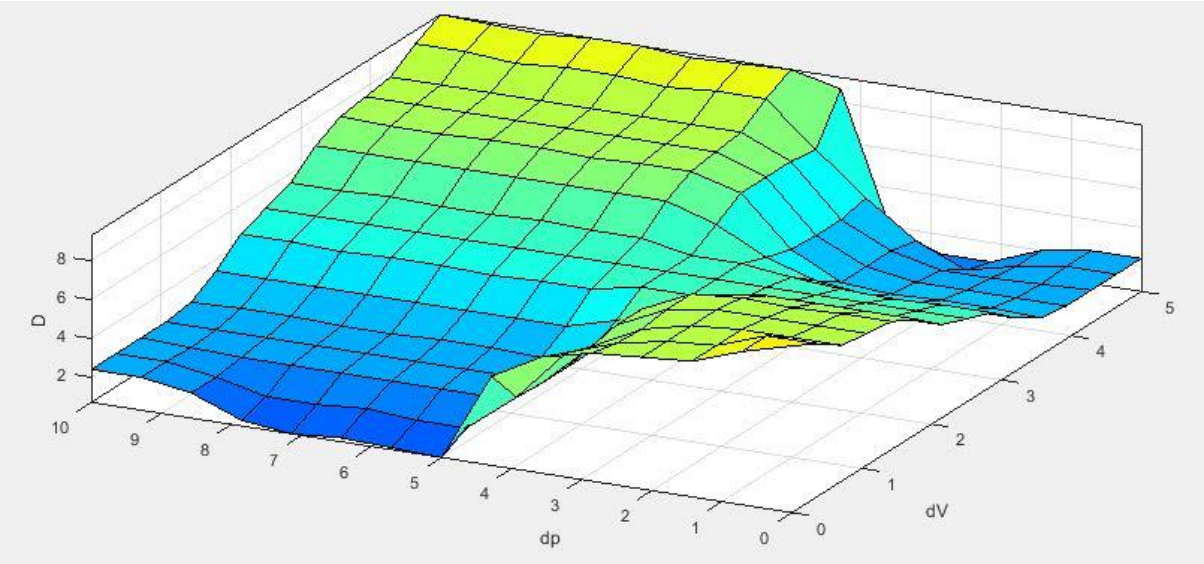

Figure 13 (b) Variation of D with changes in dP and dV using Centroid defuzzifier.

From these surface plots it could be seen that the system output duty cycle (D) exhibits smoother changes under centroid than MOM methods of defuzification.
Despite the abrupt output transitions in MOM defuzzifier, it performs better than Centroid method in 8 bit microcontroller, hence, it is the choice defuzification method in this work.
In figure 4.2(a) and (b) below, it can be seen that when there is change in the fuzzy input to the system, only one rule is fired. Which is the rule saying that everything is normal? This causes the D to settle at the middle value of five (interpreted as the level shifted zero). However, figure 4.3(a) and (b) shows an instance in the operation when the inputs changed, the result of a combination of the slight positive change in voltage - dV and power dP can be seen to have resulted in a positive change in duty cycle - D. This positive change in D will result in increased output power from the solar panel. The controller then uses perturb and observe algorithm to find the new maximum power point of operation. The output from Fuzzylite confirmed the workability of the selected rules.

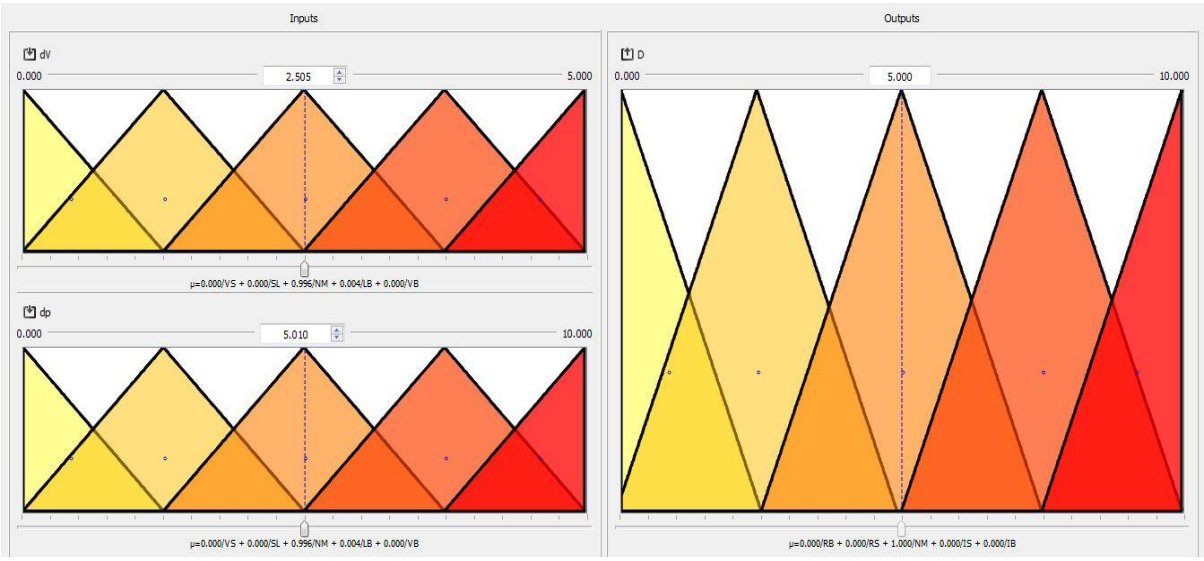

Figure 14 (a) Fuzzylite simulation showing input instance of unchanged voltage dV and power dP

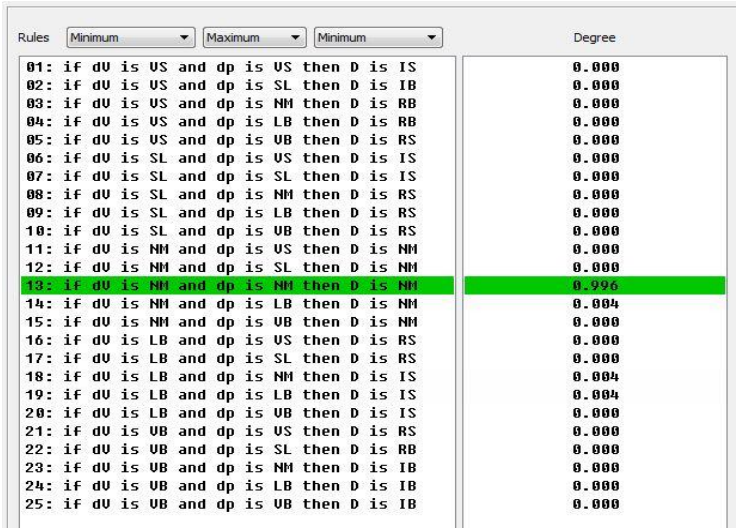

Figure 4.2 (b) Rules fired by the Fuzzylite simulation of the normal input instance.

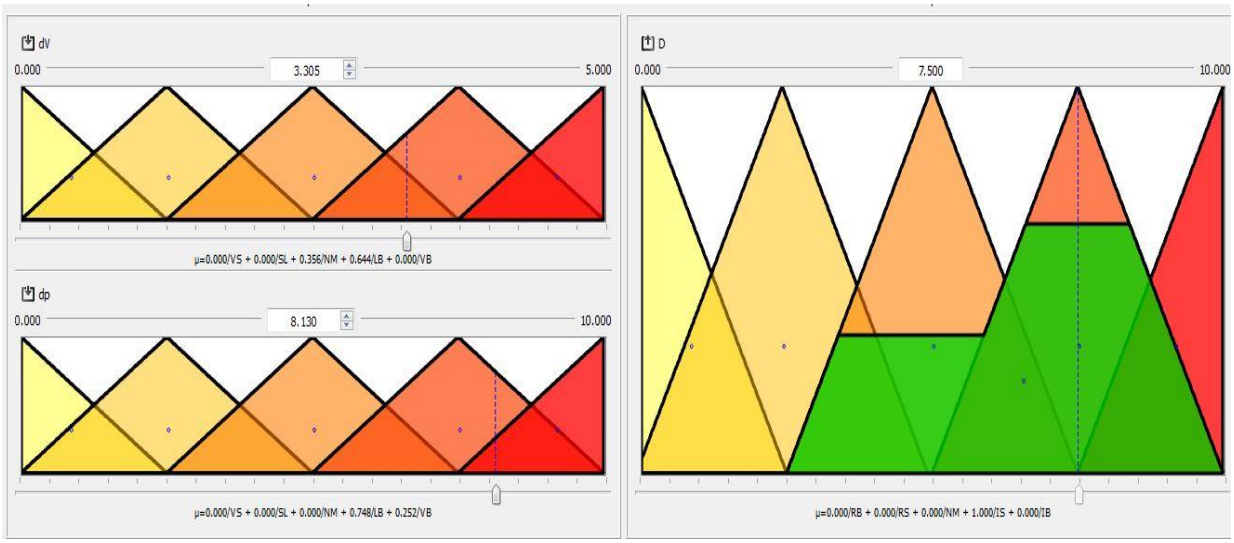

Figure 15 (a) Fuzzylite simulation showing input instance of changed voltage dV and power dP.

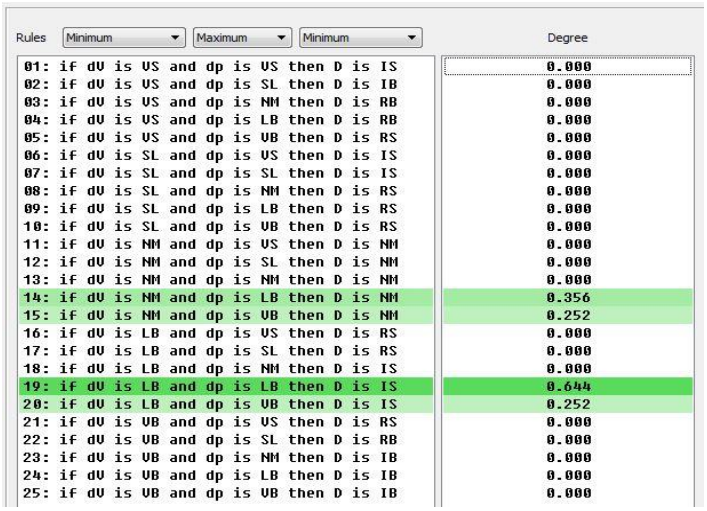

Figure 15 (b) Rules fired by the Fuzzylite simulation of the normal input instance.

MPLAB RESULTS

Coding and debugging was done in MPLAB IDE. The resulting C code shown in appendix III below, is the result of work done.

Simulation was done here for debugging and code correction purposes, before actual embedding into the microcontroller. Effort made to streamline the code for efficient operation in an 8 bit platform paid off, and the code ran as designed.

4.4. PROTOTYPE TEST RESULTS

The test result from the completed prototype (shown in figure 4.4 below) is presented here below. The test setup is shown in figure 4.5 below. A 260W solar panel was used for the test. The parameters of the solar panel are as shown in earlier. .

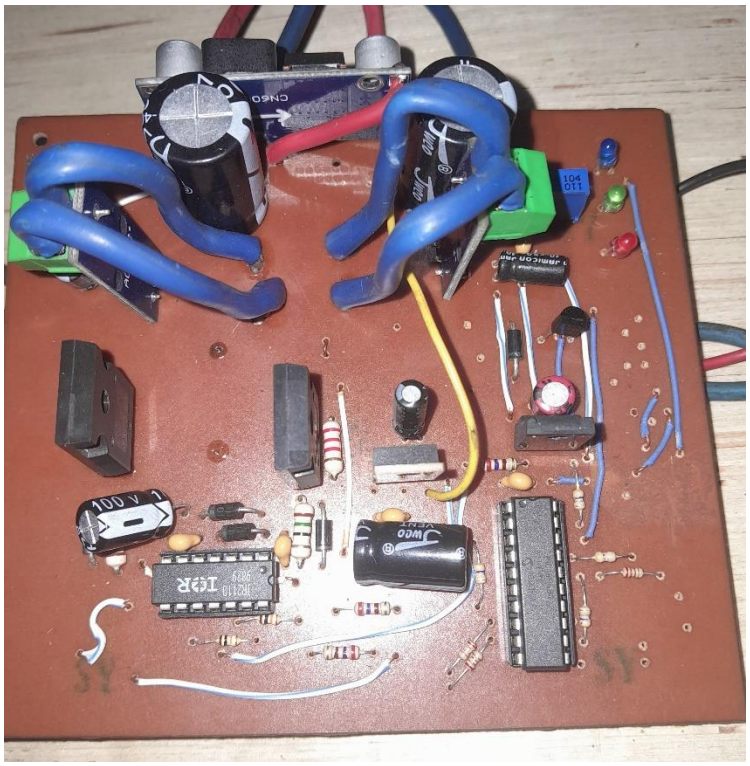

Figure 16 The Completed System board of the MPPT Charger Controller based on FuzzyLogic

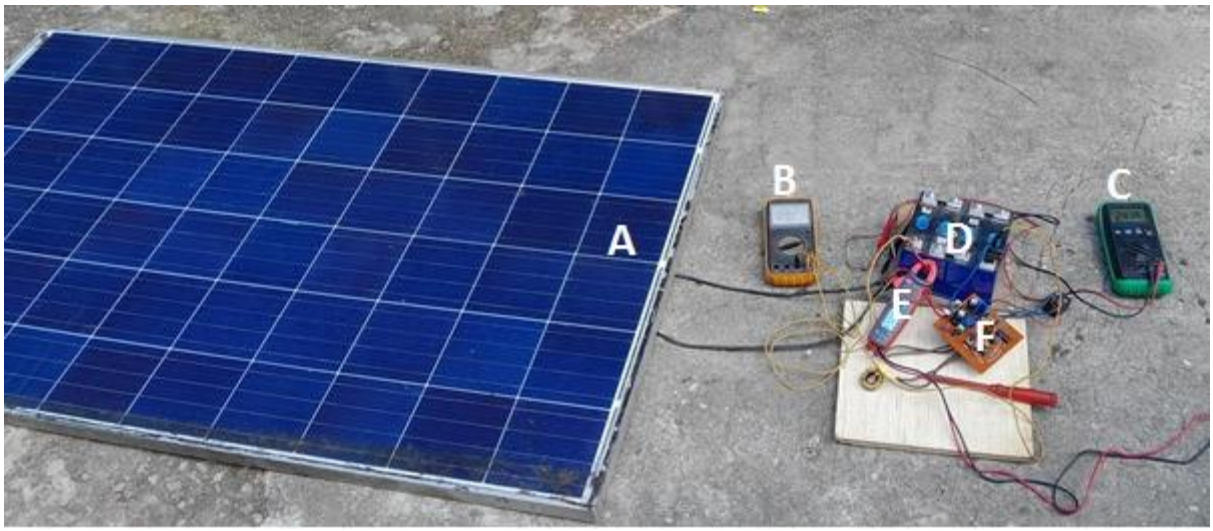

Figure 17 The Systemtest setup, (A) 260W Solar panel (B) Battery voltmeter (C) PV Voltmeter (D) Test Battery (E) PV Current meter (F) MPPT Board under test.

Several samples were collected and shown in Table 9 below. The data shown indicate different battery state of charge (SOC) and solar irradiation. Variations in solar irradiation resulted in a varying output power from the solar panel, hence varying battery charging power.

Table 9 Test Result of the MPPT Charger Controller Prototype

S/N	PV Voltage (Vpv)(V)	PV Current (Ipv)(V)	PV Power (Vpv*Ipv)(W)	Battery Voltage (V)	Battery Charge Current(A)	Battery Charging Power(W)	System Efficiency (Ƞ)
1	24.37	0.55	13.4035	13.33	0.83	11.0639	83%
2	30.50	5.96	181.78	13.50	12.22	164.97	91%
3	30.60	5.45	166.77	13.51	11.24	151.8524	91%
4	30.60	5.22	159.732	13.50	10.72	144.72	91%
5	30.20	4.22	127.444	13.48	9.00	121.32	95%
6	19.20	6.69	128.448	13.44	9.09	122.1696	95%
7	19.30	6.84	132.012	13.45	9.16	123.202	93%
8	19.30	6.89	132.977	13.46	9.19	123.6974	93%

The above results in table 9 were taken during the bulk battery charging stage. This is the stage during which the MPPT mode is operational.A maximum average system power conversion efficiency of 91% was observed during the tests. It can be seen that the PV voltage was actively altered by the MPPT charge controller with corresponding changes in PV output current, so as to extract the maximum power available at the persisting solar irradiation.

VI. Conclusion

Variations in solar irradiation resulted in a varying output power from the solar panel, hence varying battery charging power. A maximum average system power conversion efficiency of 91% was observed during the tests. It can be seen that the PV voltage was actively altered by the MPPT charge controller with corresponding changes in PV output current, so as to extract the maximum power available at the persisting solar irradiation. The project is a viable one that has commercialization potential. It improves on the local content as it is done locally. It is economical. The implementation of the project improves on the skill of the local engineers.

REFERENCES

[1]. ABONYO, C .W. (2016). MICROCONTROLLER BASED MPPT CHARGE CONTROLLER. Project report submitted in partial fulfilment of the requirement for the award of the degree of Bachelor of Science in ELECTRICAL AND ELECTRONICS ENGINEERING from the University of Nairobi 2016

[2]. Ahmad, S., Herri, G., Sri, P.& Endah, K. (2018). Modeling and Simulation of Fuzzy Logic based Maximum Power Point Tracking (MPPT) for PV Application. International Journal of Electrical and Computer Engineering (IJECE) Vol.8, No. 3. Pp. 1315-1323.

[3]. Akpado, K., Nwankwo, P., Onwuzulike D. & Orji, M. (2018). A Hybrid Approach for Air Conditioning Control System with Fuzzy Logic Controller. International Journal of Engineering and Applied Sciences (IJEAS). 5(8) DOI: 10:31873/ijeas.5.8.01 August 2018.

[4]. Akpado, K., Okwaraoka, C. & Aririguzo, M. (2017). Design and Implementation of Battery Charge Controller Using Embedded Fuzzy Logic System. International Journal of Innovative Research in Science, Engineering and Technology. Vol. 6, issue 6, June 2017.

[5]. Algarin, C.R., Giraldo, J.T. & Alvarez, O.R. (2017). Fuzzy logic based MPPT controller for a PV system. Energies 10(12), 2036, 2017.

[6]. Amrouche, B., Bechemel, M., & Guessoum, A. (2017) Fuzzy Logic based MPPT controller for a PV system. Revue des Energies Renouvelables ICRESD-07 Tlemcen (2017) 11 – 16

[7]. Carlos, R., John, T.& Omar, R. (2017). Fuzzy Logic Based MPPT Controller for a PV System. MDPI Energies 2017,10, 2036; doi: 10.3390/en10122036

[8]. Chendi, L., Yuanrui, C., Dongbao, Z., Junfeng, L., & Jun, Z. (2016). A High-Performance Adaptive Incremental Conductance MPPT Algorithm for photovoltaic Systems**.** Energies 2016, 9, 288.

[9]. Davish, M. & Namita, J. (2015). Analysis of PV Array Solar Energy Using Advanced Hill Climbing Controller International Journal of Science, Engineering and Technology Research (IJSETR), Volume 4, Issue 4, April 2015.

[10]. Dmitry, B., Saad, T., Yoash, L. & Juri, B. (2019). Improved Fractional Open Circuit Voltage MPPT Methods for PV Systems. *Electronics* **2019**, *8*, 321; doi:10.3390/electronics8030321

[11]. Donald Schelle and Jorge Castorena, Buck-Converter Design Demystified**,** Maxim Integrated Products, Sunnyvale, Calif, Power Electronics Technology, June 2006.

[12]. Farzad, S., Ali, N., Mohammad, A., Sehraneh, G. & Mehdi, A. (2012). PV Maximum Power-Point Tracking by Using Artificial Neural Network. Mathematical Problems in Engineering, Hindawi, vol. 212, pages 1-10, March 2012.

[13]. Ghazanfari, J. & Farsangi, M. (2013). Maximum Power Point Tracking using Sliding Mode Control for Photovoltaic Array. *Iranian Journal of Electrical & Electronic Engineering, Vol. 9, No. 3, Sep. 2013*

[14]. Hasan, M., Mekhilef, S. & Metselaar, I. (2013). Photovoltaic System Modeling with Fuzzy Logic Based Maximum Power Pin Tracking Algorithm. International Journal of Photoenergy Volume 2013. Article ID 762946

[15]. Hellmann, M. (2001). Fuzzy logic introduction. Universite de Rennes, vol.1, pp. 1-9, 2001.

[16]. Ibrahim, I. & Abdelmeneim, A. (2018). Using Intelligent Control to Improve PV Systems Efficiency. arXiv:1802.03463 (physics) 2018.

[17]. Jemaa, A., Zarrad, O., Aurelian, C. &Mihai, P. (2016). Comparison of Fuzzy and Neuro-Fuzzy Controllers for maximum Power Point Tracking of Photovoltaic Modules. International Conference on Renewable Energies and Power quality (ICREPQ'16) Madrid (Spain) Vol.1, No 14.

[18]. Javadi, S. (2020). Fuzzy Control. Islamic Azad University Central Tehran Branch.

[19]. Karthika,S., Velayutham,K., Rathika, P., & Devaraj, D. (2014). Fuzzy Logic Based Maximum Power Point Tracking Designed for 10KW Solar Photovoltaic System with Different Membership Functions. World Academy of Science, Engineering and Technology International Journal of Electrical and Computer Engineering Vol: 8, No 6.

[20]. Mostefa, K., & El Madjid, B. (2017). Artificial intelligence-based maximum power point tracking controllers for Photovoltaic systems: Comparative study. Renewable and Sustainable Energy Reviews 69 (2017) 369–386. journal homepage: www.elsevier.com/locate/rser.

[21]. Mppt-solar-charge-controllers. (2023, 4, 3). Retrieved from NAZ solar electric: http://www.solar-electric.com/learning-center/mppt-solar-charge-controllers.html/

[22]. Renewable energy(2022,12, 8). Retrieved from www.nrdc.org/stories/renewable-energy-clean-facts#see-whatis

[23]. Samosir**,** A**.**, Gusmedi, H., Purwiyanti, S. &Komalasari, E. (2018). Modeling and Simulation of Fuzzy Logic based Maximum Power Point Traking (MPPT) for PV Application. International Journal of Electrical and Computer Engineering (IJECE) Vol. 8, No. 3, June 2018, pp. 1315-1323.

[24]. Volkan, Y. & Kadir, A. (2017). Maximum Power Point tracking in Solar Power Systems by Using Differential Evolution Methods with Embedded system. International Journal of Engineering Research and Development volume: 9, issue: 3 .

[25]. Yiwang, W., Yong, Y., Gang, F., Bo, Z., Huiqing, W., Houjun, T., Li, f., & Xiango, C. (2018). An Advanced Maximum Power Point Tracking Method for Photovoltaic Systems by Using variable Universe Fuzzy Logic Control Considering Temperature Variability. Electronics 2018, 7,355; doi: 10.3390/electronics7120355.

[26]. Zadeh, L.A. (1994). Fuzzy logic: Issues, Contentions And Perspectives. University of Caliornia, Berkeley, CA 94720: IEEE.